Corrosion Science 51 (2009) 2266–2278

Contents lists available at ScienceDirect

Corrosion Science

journal homepage: www.elsevier.com/locate/corsci

Artificial neural network corrosion modeling for metals in an equatorial climate

Elaine D. Kenny *, Ramón S.C. Paredes, Luiz A. de Lacerda, Yuri C. Sica, Gabriel P. de Souza, José Lázaris

Rua Mamoré, 20 Residencial Iguaçu, Alphaville Graciosa, CEP: 83327-086, Pinhais, Paraná, Brazil

Universidade Federal do Paraná, Setor de Tecnologia, Departamento de Engenharia Mecânica, Centro Politécnico, Jardim das Américas, CEP: 81531-990, Caixa-postal: 19011, Curitiba, Paraná, Brazil

ARTICLE INFO

Article history:
Received 5 January 2009
Accepted 5 June 2009
Available online 13 June 2009

Keywords:
B. Artificial neural network
C. Atmospheric corrosion

ABSTRACT

The majority of the metals used in the distribution and transmission electric energy lines, such as cables, towers and accessories are susceptible to the corrosion degradation process. For that reason, studying the factors that influence the atmospheric corrosion is an important issue. In this paper, an artificial neural network model was developed with linear and sigmoidal functions, aiming to predict low-carbon steel, copper and aluminum corrosion rates according to environmental parameters in the area of São Luis – Maranhão, Brazil. The area along the "702 – São Luis II –Presidente Dutra" 500 kV transmission line, located in an equatorial region, is employed for this purpose. A specific methodology was developed to determine the local corrosivity rate for these metals. Five atmospheric corrosion stations (ACS) were installed along the 702 transmission line in an extension of 200 km. Along with the meteorological data, local pollutants were collected and analyzed during a period of two years. In the same period, specimens were exposed to this atmosphere and periodically collected for corrosion evaluation. The obtained results indicate that the neural network can be used as a good corrosion estimator.

1. Introduction

It is well known that the corrosion rates of metals exposed to the atmosphere can vary as much as a hundred times depending on the aggressiveness of the environment. For this reason, it is justified the interest in monitoring the fundamental agents that take part in the atmospheric corrosion process. The different influencing parameters cause a wide dispersion of the results and the interpretation of the collected data is not straightforward. The complexity and non-linearity of the physical–chemical processes occurring in the atmospheric corrosion phenomenon [1] make predictions about corrosion rates a very difficult task. Therefore, the analytical and numerical models developed for estimating corrosion speed in metals exposed to the atmosphere can be very useful. These tools may provide means for the assessment of the metallic structures useful life and the costs associated to their degradation. Also, they may help understanding the kinetics of the atmospheric corrosion process and the weight of each involved environmental parameter.

Great part of the models used for predictions are statistical regression models that adjust specific mathematical functions to the given data minimizing the sum of the square of the differences between measurements and the estimating function. These models have demonstrated being effective in restricted areas [1,2], but are limited when available corrosion information is highly non-linear [3–5]. Thus, generalized mathematical models are necessary to predict the atmospheric corrosion rates in different climates and contamination degrees [6].

For this reason a mathematical model based on an artificial neural network is proposed in this work, taking into account the experimental data of corrosion rates of the metal exposed to natural weathering, and the corresponding atmospheric characteristics monitored in different sites.

Artificial neural networks are an efficient numerical tool, inspired in biologic neuronal systems, which can be used to perform computing simulations. They can be used to model and characterize atmospheric corrosion processes based on experimental observations. The networks can be designed and trained to estimate corrosion rates of metallic materials, from a group of relevant environmental parameters and material data.

The networks are composed by basic interconnected elements called neurons and, just like in nature, its capacity is strongly influenced by its topology. In other words, by the number and type of connections between neurons [7,8]. Input information travel through connectors (synapses) and are received by neurons. In each neuron the received impulses are processed, modulated and

* Corresponding author. Address: Rua Mamoré, 20 Residencial Iguaçu, Alphaville Graciosa, CEP: 83327-086, Pinhais, Paraná, Brazil. Tel.: +55 41 35511251; fax: +55 41 33613123.

E-mail addresses: elainekenny7@yahoo.com.br (E.D. Kenny), ramon@demec.ufpr.br (R.S.C. Paredes), alkimin@lactec.org.br (L.A. de Lacerda), yuri.sica@gmail.com (Y.C. Sica), gabpinsou@uol.com.br (G.P. de Souza), lazaris@yahoo.com.br (J. Lázaris).

0010-938X/$ - see front matter © 2009 Elsevier Ltd. All rights reserved.
doi:10.1016/j.corsci.2009.06.004

passed ahead. In the artificial neuron entries are numerical values which represent information passed from other neurons (a_1, a_2, ..., a_n) and weighted according to the connection intensities (w_1, w_2, ..., w_n). The sum of these values plus a bias composes a single entry value, as illustrated in Fig. 1. The entry value can be modulated with different transfer functions $f()$, which must be selected according to the nature of the problem.

Once the topology of an artificial neural network and the modulating neuron functions are chosen the network can be trained to execute specific tasks through the definition of its connections. Mathematically, this definition is characterized by numerical values associated to each connection, weighting the importance of the transmitted signal.

Usually, network training is done with an amount of known information related to the task or objective of the network. Information is summarized by input and output parameters. Training is conducted in such a way that input values result in output values similar to the measured or observed ones. Training quality is directly proportional to the availability of input/output data. The training process of a neural network is presented in Fig. 2.

Topology of an artificial neural network can assume different levels of complexity. However, it is common to use feedforward type networks, which are normally composed by an initial layer of neurons with the exclusive task of receiving and transmitting entry values; one or more internal layers of neurons with linear or non-linear sigmoidal modulating functions; and an output layer of neurons linearly modulated. The number of neurons in the input and output layers are dependent on the problem and the number of adopted influence parameters. Multiple intermediate neuron layers with non-linear modulating functions allow the network to learn linear and non-linear relations between input and output parameters [9,10].

In this work a multilayer perceptron artificial neural network model was employed with linear and sigmoidal tangent and logarithmic transfer functions, aiming to predict low-carbon steel, copper and aluminum corrosion rates. Detailed environmental data from the studied region, where the "702 – São Luís II – Presidente Dutra" transmission line is situated, was introduced in the model of analysis. The neural network is a feedforward type with a Levenberg–Marquardt backpropagation training algorithm. All steps of data preprocessing and network training were implemented in a MatLab® (version 6.5) algorithm.

2. Experimental

Environmental parameters were used as entry values in the adopted artificial neural network and the laboratory evaluated corrosion rates from metallic materials exposed to the atmosphere were used as target data in order to train the network. These data were collected from five Atmospheric Corrosion Stations (ACS) located along the 500 kV "Presidente Dutra" transmission line, which is 200 km long and is situated in the southern part of Sao Luis (see Fig. 3). In the ACS, besides continuous environmental monitoring, representative metallic specimens for the aerial components were placed in racks and exposed to the atmosphere for almost two years. In this period, specimens were periodically collected and examined for corrosion.

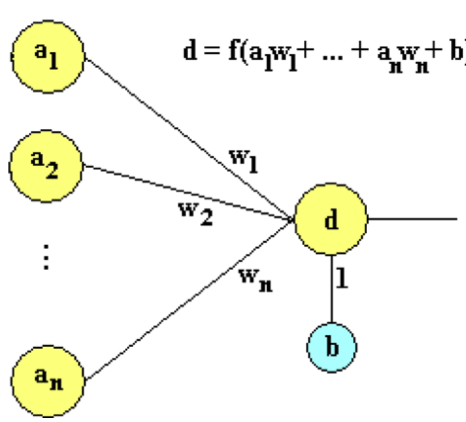

Fig. 1. Processing information scheme of a single artificial neuron.

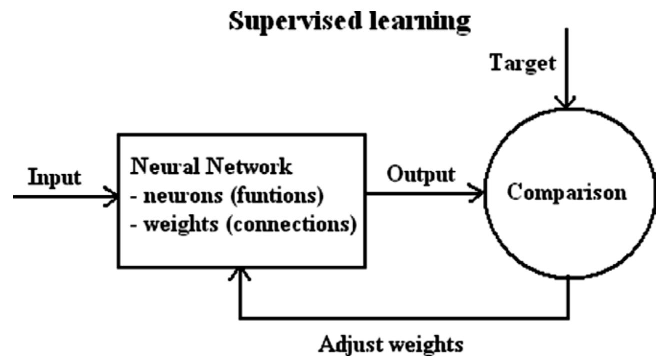

Fig. 2. Supervised learning scheme of a neural network.

In order to study the local atmospheric corrosivity, the following environmental parameters were monitored: airborne salinity represented by chloride ions Cl^-, sulfur-containing substances represented by SO_x ions, dustfall deposition rate, temperature, relative humidity, time of wetness, daily precipitation, solar radiation and wind speed. These parameters were assumed to be the main responsible for the local atmospheric aggressiveness and their levels were determined monthly.

In order to visualize the aggressiveness of the pollutants in the area covered by the ACS, data from particle deposition, Cl^- and SO_x ions were mapped according to their average concentration in chosen periods with a georeferential extrapolation tool. The geoprocessing software – ArcView 9.0 GIS (Geographic Information System) was used for this purpose. In this mapping analysis, vectorial and punctual layers were defined and interpolated by the deterministic interpolating method called IDW (Inverse Distance Weighted) [11]. IDW is a geospatial analysis resource available on the ArcView software module Spatial Analyst. It is based on the weighted multiple linearity combination of the pollutants average concentrations determined in each ACS. The weighting factor is the inverse of the distance between data points and provides a continuous surface named atmospheric corrosivity raster [12].

2.1. Atmospheric corrosion stations – installation and monitoring

Based on the corrosion problems detected along the 500 kV "Presidente Dutra" transmission line, five ACS were installed for the atmospheric corrosion monitoring. Their locations were defined by the local Energy Company, taking into account the history of faults caused by the intense corrosion of transmission line components and the high maintenance costs of the network. Vandalism was also considered in this evaluation. As a result, five pylons were selected and the pollutants collectors and racks with metallic specimens were installed 15 m high above the ground.

The collectors were installed to determine the concentration of chloride and sulfate ions in the atmosphere according to ABNT NBR 6211 [13] and ABNT NBR 6921 [14] standards, respectively. Dustfall deposition rate was measured according to ASTM D 1739 [15]. Corrosion rate of the metallic specimens exposed in the racks was evaluated according to ABNT NBR 6209 [16]. Table 1 shows

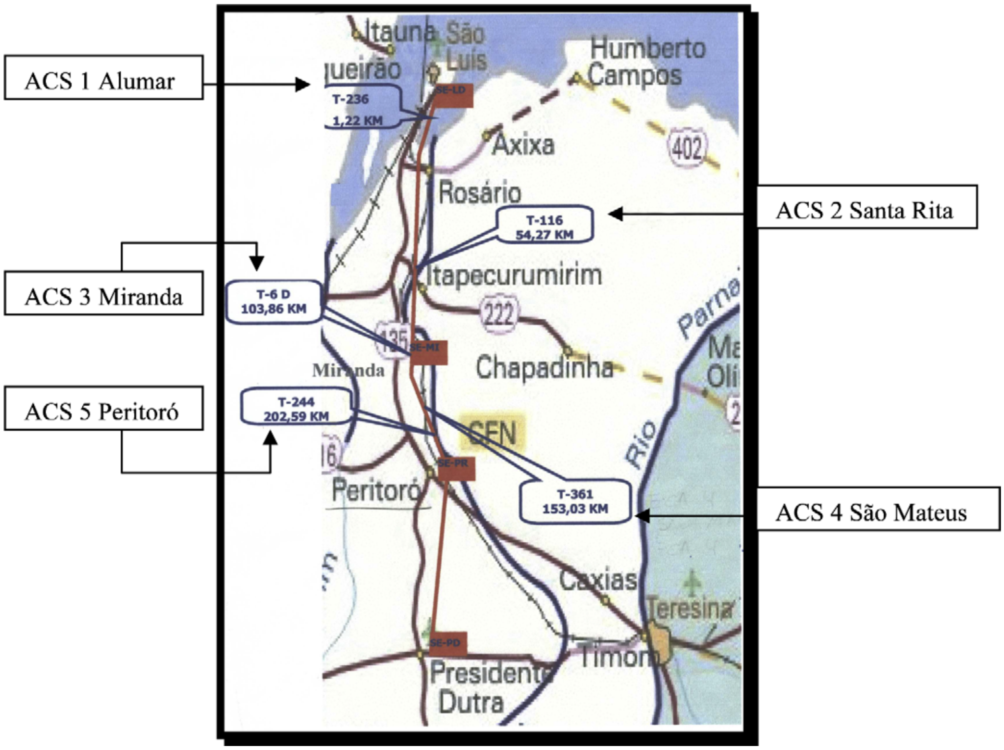

Fig. 3. Map with the "702 – São Luís II – Presidente Dutra" transmission line and ACS sites location.

ACS locations, data of installation and type of pollutant collector devices.

In Table 1, it can be seen that two towers were selected for having a complete ACS with weathering racks: ACS 1, located in tower T-236, close to Alumar industrial complex, which produces aluminum and, consequently, liberates high level of bauxite particulates; and ACS 3, located in tower T-6D, close to Miranda urban area.

2.2. Chloride deposition rate

Determination of the airborne salinity represented by the concentration of chloride in the atmosphere (soluble chlorides as those in aerosols from industrial or marine environments) and its deposition rate over the metallic surfaces was carried out in accordance with ABNT NBR 6211 [13], which prescribes the moist candle method. Results are expressed in mg Cl^-/m^2 day.

2.3. Sulfur compounds deposition rate

Determination of the sulfur compounds deposition rate was carried out in accordance with ABNT NBR 6921 [14], which prescribes the method for gravimetric evaluation of the sulfur-containing substances (SO_2, SO_3, H_2S and $SO_4{}^{2-}$) in the atmosphere, obtained by the oxidation or fixation on a reactive surface. Results are expressed in mg SO_2/m^2 day or mg $SO_3/100cm^2$ day.

2.4. Dustfall rate

Determination of dustfall rate was carried out in accordance with ASTM D1739 [15]. This method prescribes the collecting of atmospheric dust in a standard polymeric recipient by dissolution and sedimentation of the soluble and non-soluble particulate materials in water. The results are expressed in g/m^2 30 days of settling particulate matter in the atmosphere.

2.5. Meteorological parameters and classification of corrosivity of São Luis city atmosphere

The meteorological parameters such as temperature, relative humidity, precipitation, solar radiation and wind speed were obtained from information supplied by CPTEC [17] – Climate Studies and Weather Forecast Center. These parameters are necessary for the classification and characterization of the atmosphere corrosivity [18]. Two methodologies were used in order to classify the climate of São Luis city: Köppen and Brooks. These methodologies are described in Morcillo et al. [19].

2.6. Natural weathering

The studied materials, low-carbon steel, 6351 aluminum-alloy and electrolytic copper were prepared in specimens with

Table 1
ACS modules installed in São Luis.

ACS	Date of installation	Location	Collecting devices
ACS 1	05.07.2004	Alumar-T-236	Chlorides; sulfates; dustfall and natural weathering rack
ACS 2	05.11.2004	SantaRita-T-116	Chlorides and sulfates
ACS 3	05.12.2004	Miranda-T-6D	Chlorides; sulfates; Dustfall and Natural weathering rack
ACS 4	05.13.2004	São Mateus-T-361	Chlorides; sulfates and dustfall
ACS 5	05.13.2004	Peritoró-T-244	Chlorides and sulfates

$10 \times 5 \times 0.3$ cm size in accordance to ABNT NBR 14643 [18] .They were identified, degreased in acetone, rinsed, dried and weighted in laboratory. They were fixed on racks, as shown in Fig. 4, which were installed at towers T-236 and T-6D for natural weathering.

The rack panels were made with galvanized steel profiles and were installed 30° from the horizontal in accordance to ABNT NBR 6209 [16]. In ACS 3 the panel was installed facing the geographic north in order to receive more sunlight on the surface of the metallic samples, but in ACS 1 the panel was installed facing an industrial complex in the geographic south receiving direct influence of the pollutants given the preferential wind direction.

After a predefined period of exposition, specimens were collected and cleaned, removing the corrosion products with an appropriate procedure for each type of metal in accordance with ABNT NBR 6210 [20]. Such procedure was performed by mechanical and/or chemical processes, taking care for not removing the substrate. After cleaning, the samples that presented uniform corrosion were weighted for the mass loss and corrosion rate determination. The samples with evidence of localized corrosion, were investigated with a SMZ800 NIKON stereoscopic microscope and by metallographic analysis using a MM6 Leitz-Wetzlar optical microscope for identifying the corrosion type. In the metallographic tests samples were cut and set with bakelite, sandpapered up to 1200 grid and polished with 3 μm diamond paste.

2.7. Neural network model

The environmental parameters included in the adopted artificial neural network as entry values are listed below:

1. Time of exposure of the metallic material (days).
2. Average relative humidity in the period of exposure (%).
3. Average daily precipitation in the period of exposure (mm).
4. Time of wetness of the metallic material (days).
5. Average wind velocity in the period of exposure (m/s).
6. Average solar radiation in the period of exposure (MJ/m^2).
7. Average temperature in the period of exposure (°C).
8. Average concentration of Cl^- íons in the period of exposure (mg/m^2 day).
9. Average concentration of SO_x íons in the period of exposure (mg/m^2 day).
10. Average amount of solid particles deposition in the period of exposure (g/m^2 30 days).

The network topology was defined after a series of tests with different configurations. The adopted network for the corrosion estimate analysis can be seen in Fig. 5.

The network has the following characteristics: 10 neurons in the entry layer, one for each environmental parameter; 02

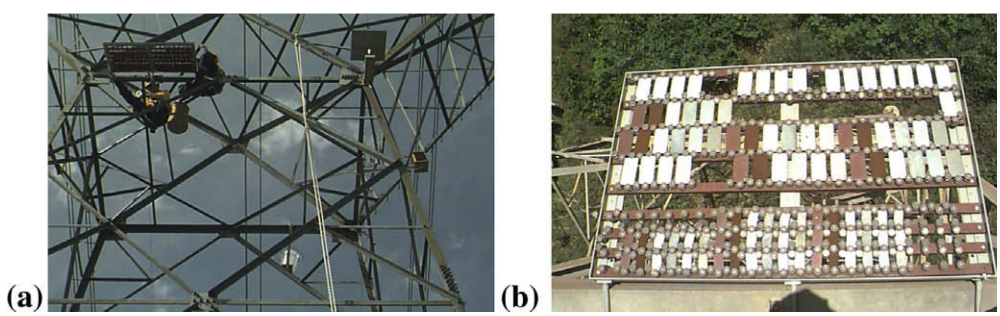

Fig. 4. Installation of the rack panel in tower T-6 D.

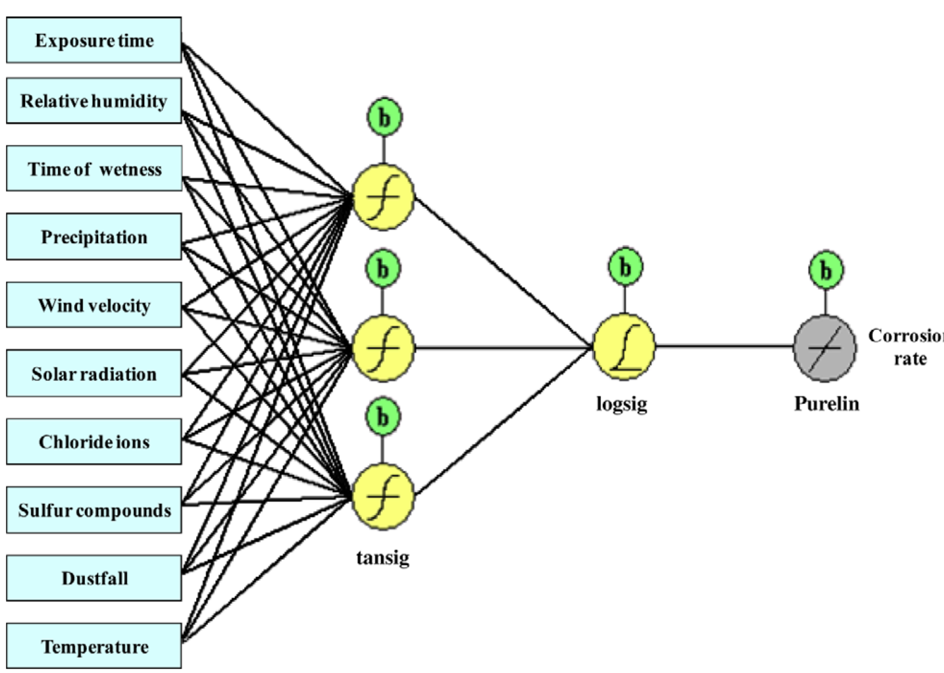

Fig. 5. Scheme of the adopted artificial neural network.

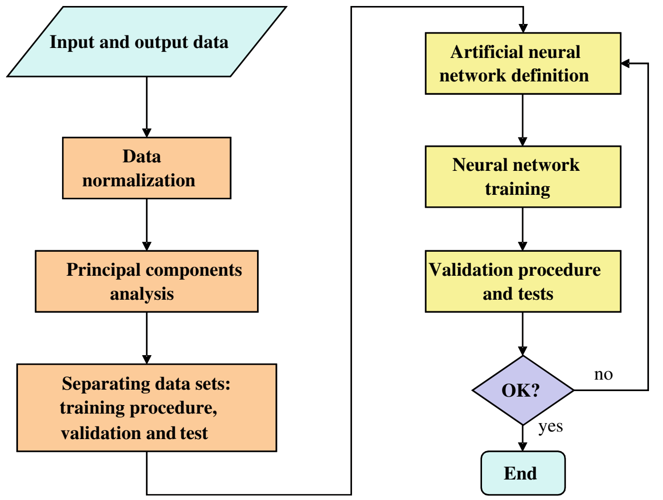

Fig. 6. Flowchart with data preprocessing and artificial neural network training.

intermediate layers of sigmoidal neurons – the first layer with tangential modulating functions (*tansig*) and the second layer with logarithmic modulating functions (*logsig*). In that way, the signal passed to the last layer is a positive number, since corrosion cannot be defined by a negative value; 01 output neuron with a linear function (*purelin*) to amplify the received signal to real corrosion rate values.

2.7.1. Training the artificial neural network

Before proceeding with the simulations to define corrosion rate from an environmental data set, the artificial neural network must be trained. In other words, the weight of each neuron connection must be defined through a learning procedure from available environmental and corrosion rate data.

Training is performed with iterative algorithms, such as back-propagation, which is the most commonly used method. In this method, a series of numerical evaluations are performed from the external layers towards the initial ones, considering the gradient of the errors to adjust the connection weights [7,10].

Preconditioning of input and output data can improve the network training process. In this work, this procedure consisted of normalizing statistical parameters of the training data, resulting in a new group of data with zeroed average and unit standard deviation. Another preprocessing technique applied to the input data was PCA (principal component analysis) with the objective of detecting redundancy in the input data. This technique may reduce the dimension of the input array, ordering data components according to their importance. It also allows discarding data depending on its percentage contribution value.

Training is evaluated by measuring the root of the mean square error between calculated results and expected output data. One common way of measuring is through a linear regression analysis.

2.7.2. Training algorithm

All steps of the neural analysis including data preprocessing, artificial neural network definition and training were assembled in a MatLab algorithm, according to the flowchart in Fig. 6. Observe that the training procedure is repeated until predefined criteria are satisfied.

The backpropagation algorithm used for training the network was Levenberg–Marquardt, which presented the best performance in the search for the weights of neuron connectors.

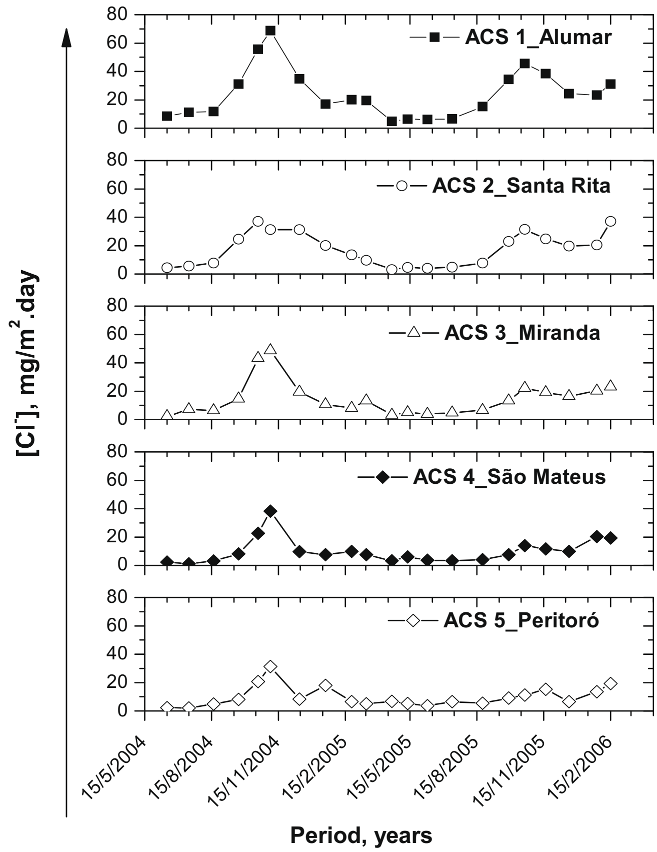

Fig. 7. Chloride deposition rates for each ACS.

3. Results and discussion

3.1. Meteorological data

Based on the available meteorological data [17,21], the climate of São Luis city is classified as equatorial –Am, according to Köppen. It is controlled by the tropical and equatorial air masses, being basically hot and humid and characterized by two defined seasons: the dry period (July–December) and the rainy period (January–June). In Table 2, the seasonal averages for the monitored meteorological parameters are presented.

It can be observed that the annual average temperature of São Luis city is (28 ± 2) °C with high relative humidity, with average values ranging from 80 to 92%. Such high humidity increases corrosion probability of the exposed metals due to the formation of a thin electrolyte film on the substrate where pollutants are kept. On the other hand, the rain is usually responsible for the leaching of the atmospheric pollutants deposited on the surface of the me-

Table 2
Meteorological parameters of São Luis city (seasonal averages – dry and rainy periods).

Period	Temperature (°C)	Relative humidity (%)	Precipitation (mm/month)	Solar radiation (cal/cm^2 day)	Insolation (hours/month)	Evaporation (mm)	Wind Velocity (m/s)	Pressure (mbar)
Jan–June	26.5	92.0	281	331.4	150.7	59.6	5.5	1006
July–Dec	30.0	80.0	13	448.0	241.6	110.3	7.0	1006

Table 3
Chloride deposition average during dry and rainy seasons.

Period	Chloride deposition rate (mg/m^2 day)				
	ACS 1	ACS 2	ACS 3	ACS 4	ACS 5
July–Dec/2004	35.56 ± 9.47	22.92 ± 5.41	23.31 ± 7.48	13.86 ± 5.78	12.56 ± 4.56
Jan–June/2005	12.33 ± 2.96	9.19 ± 2.72	7.36 ± 1.63	6.34 ± 1.02	7.57 ± 2.15
July–Dec/2005	27.41 ± 6.03	18.58 ± 4.20	13.79 ± 2.82	8.35 ± 1.71	9.01 ± 1.53
Jan–Feb/2006	27.32 ± 3.87	28.82 ± 8.30	21.73 ± 1.48	19.81 ± 0.44	16.44 ± 2.94
Average	26.86 ± 4.17	19.36 ± 2.75	16.48 ± 2.97	11.48 ± 2.09	11.16 ± 1.71

tal, which may decrease the electrolyte concentration and, consequently, the corrosion rate. This is observed in the period between January and June, where the monthly accumulated precipitation is 280 mm, approximately.

The average accumulated solar radiation in the rainy period is about 331.4 cal/cm^2 day, but the highest average is in the dry period, about 448.0 cal/cm^2 day. This fact influences directly the time of wetness (tow) on the metal and the corrosion rate due to the

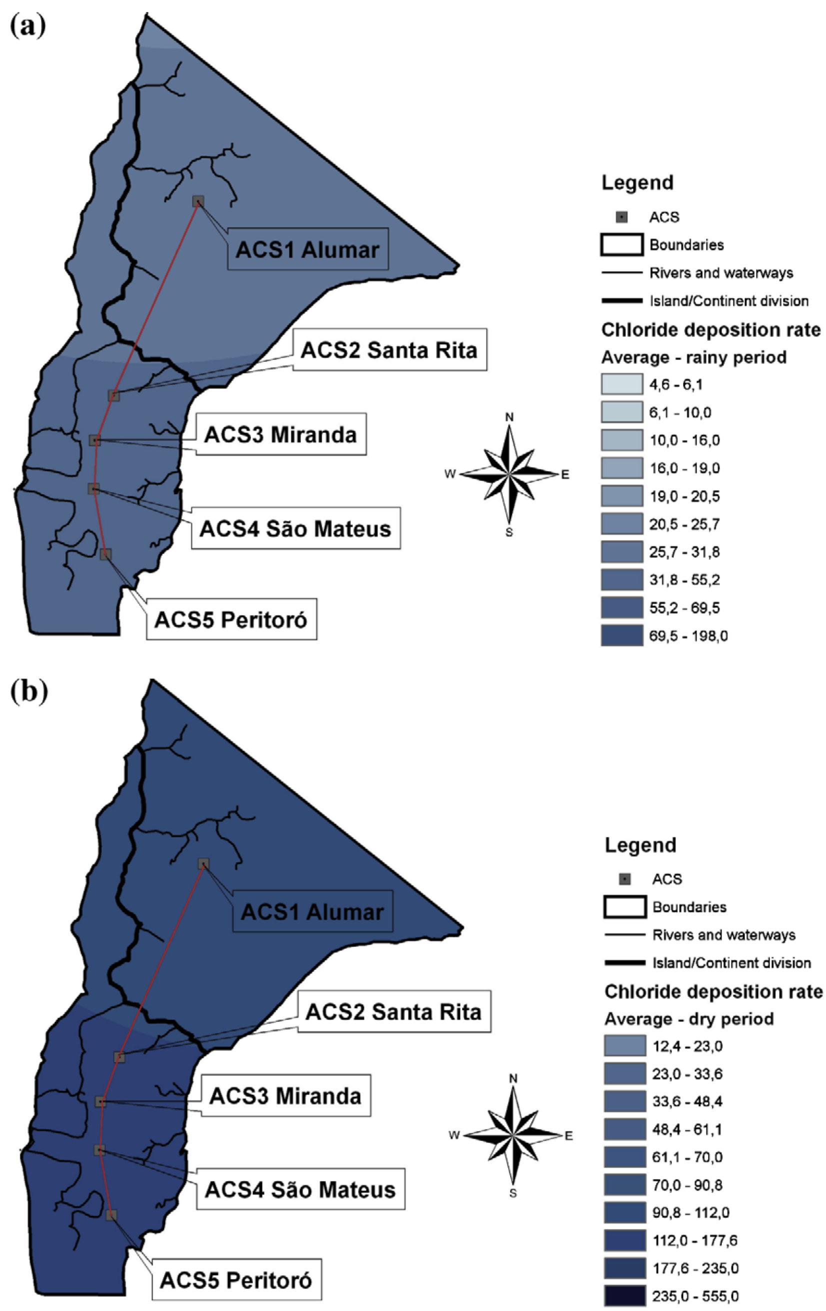

Fig. 8. Chloride deposition rate maps along the transmission line area in São Luis-MA, in mg/m^2 day: (a) rainy season; (b) dry season.

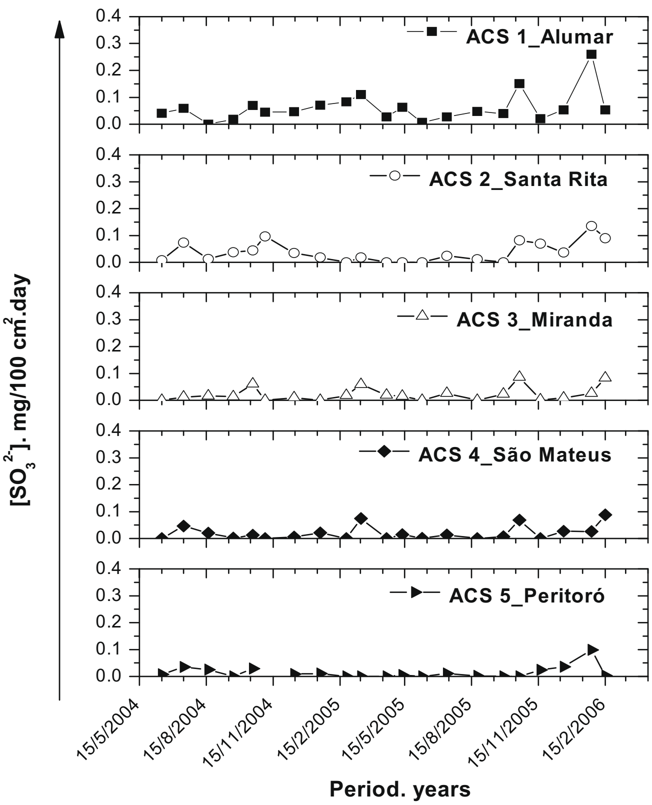

Fig. 9. Sulfur compounds deposition rate in each ACS.

semi-conducting behavior of the oxides formed by the corrosion products.

The tow annual average is approximately 4400 h, which classifies São Luis atmosphere as "τ4" corrosivity category, i.e. highly corrosive atmosphere. The deteriorating index of the atmosphere (Id) calculated by Brooks expression [19] is 4.7, which classifies São Luis atmosphere as corrosive with a moderate deterioration degree.

3.2. Chloride deposition rate

The chloride deposition rates, monitored in each ACS, are plotted in Fig. 7.

It can be seen that only ACS 1 – Alumar can be classified as a typical marine environment, given the aggressive atmosphere resulting from the airborne salinity in Liesegang apud Kenny [13] classification. However, ACS 2 – Santa Rita could also be classified as marine environment if only the dry season is considered. The average values in each ACS during the dry and rainy seasons are presented in Table 3.

It can be observed that the chloride deposition rate is much higher in the dry season, which can be explained by the higher ocean evaporation rate, contributing to carrying the particles for a longer distance. Also, the deposits of salts are very soluble in the rainwater.

Fig. 8 shows the contour maps of chloride deposition rate for the rainy (a) and dry (b) seasons along the transmission line area in Sao Luis-MA respectively. These maps were obtained through georeferencial extrapolation from the ACS values.

3.3. Sulfur compounds deposition rate

The sulfur dioxide deposition rates monitored in each ACS are plotted in Fig. 9.

The average values in each ACS, during the dry and rainy seasons are presented in Table 4.

According to these average results, all stations can be classified as low to medium aggressivity, except in 2006 when ACS 1 – Alumar and ACS 2 – Santa Rita reached an urban environment aggressiveness.

Fig. 10 shows the contour maps of sulfur dioxide deposition rate for the rainy and dry seasons along the transmission line area in Sao Luis-MA, respectively. These maps were obtained through georeferencial extrapolation from the ACS values.

3.4. Settleable particulate matter (SPM)

Average values of settleable particulate matter are shown in Table 5.

The highest dustfall rates were registered in ACS 1 – Alumar, which is very close to an industrial complex. Dustfall is responsible for increasing the atmosphere corrosivity due to their hygroscopic properties. It is important to consider that the greatest deposition rates of atmospheric pollutants are recorded in the dry season (July–December), when the pollutant wash-away does not occur.

3.5. Natural weathering

In Table 6, corrosion rates and thickness losses for different specimens of low-carbon steel are presented for two different sites, ACS 1 and ACS 3, as well as their classification according to ABNT NBR 14643 [18].

It can be seen that ACS 1 atmosphere is more aggressive compared to ACS 3. ACS 1 can be classified in the category "very high corrosivity degree", while ACS 3 as "medium to high corrosivity degree". The low-carbon steel specimens presented a generalized corrosion in both sites.

In Table 7, corrosion rates and thickness losses for different specimens of copper are presented for two different sites, ACS 1 and ACS 3, as well as their classification according to ABNT NBR 14643 [18].

It can be seen that both sites are classified as C_4 and C_5, which means "high to very high corrosivity degree". In Fig. 11, it is noticed that the copper specimens presented alveolar corrosion.

In Table 8, corrosion rates and thickness losses for different specimens of aluminum are presented for two different sites, ACS

Table 4
Sulfur compounds average deposition rates during dry and rainy seasons.

Period	Sulfur compounds deposition rate (mg SO_3/100 cm^2 day)				
	ACS 1	ACS 2	ACS 3	ACS 4	ACS 5
July–Dec/2004	0.040 ± 0.011	0.050 ± 0.012	0.019 ± 0.009	0.015 ± 0.007	0.020 ± 0.007
Jan–June/2005	0.060 ± 0.015	0.006 ± 0.004	0.019 ± 0.009	0.019 ± 0.009	0.003 ± 0.002
July–Dec/2005	0.056 ± 0.020	0.037 ± 0.013	0.024 ± 0.013	0.019 ± 0.011	0.012 ± 0.006
Jan–Feb/2006	0.157 ± 0.103	0.113 ± 0.023	0.054 ± 0.028	0.057 ± 0.031	0.051 ± 0.048
Average	0.061 ± 0.012	0.038 ± 0.009	0.023 ± 0.006	0.020 ± 0.006	0.015 ± 0.005

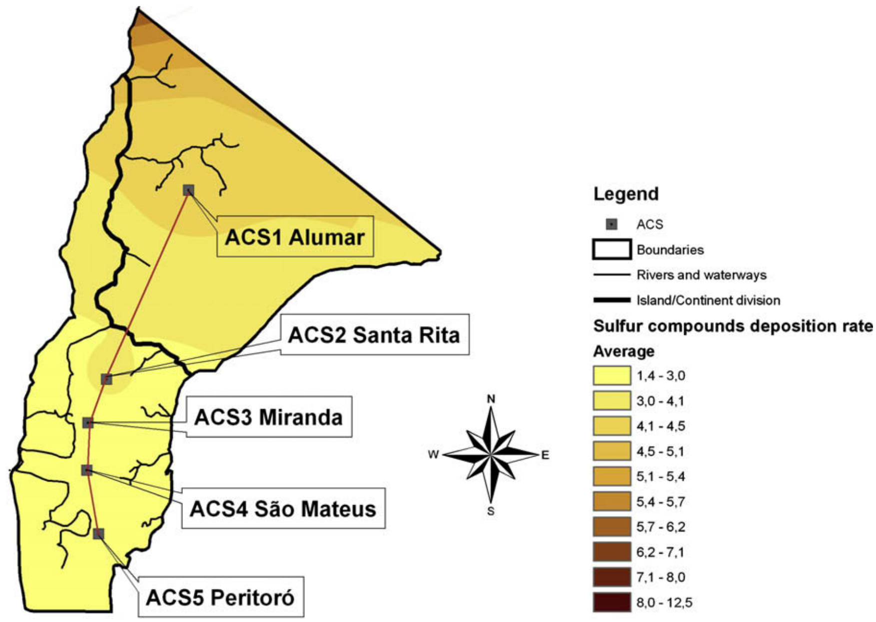

Fig. 10. Sulfur compounds deposition rate maps along the transmission line area in Sao Luis-MA, in mg SO_2/m^2 day.

Table 5
Settleable particulate matter average rates during dry and rainy seasons.

Period	Setteable particulate matter (g/m^2 30 days)		
	ACS 1	ACS 3	ACS 4
July–Dec./2004	4.47 ± 0.51	2.30 ± 0.29	2.57 ± 0.35
Jan.–June/2005	3.88 ± 0.73	3.01 ± 0.66	1.93 ± 0.60
Average	4.18 ± 0.62	2.66 ± 0.48	2.25 ± 0.47

1 and ACS 3, as well as their classification according to ABNT NBR 14643 [18].

It can be seen that ACS 1 is classified between as C_3 and C_4, which means "medium to high corrosivity degree", while ACS 3 presents a lower corrosivity, ranging between C_2 and C_3 categories. The aluminum specimens have shown localized corrosion in both sites. However, it can be seen in Fig. 12 that specimens in ACS 1 presented more (and deeper) pits.

Table 6
Corrosion rate, thickness loss and atmosphere corrosivity degree – low-carbon steel.

Corrosion site	Code	Photo after 21 months of exposure	Exposure time		Corrosion rate		Thickness loss (μm)	Corrosivity degree
			Days	Months	(μm/year)	(g/m^2 year)		
ACS 1 Alumar	A 16		104	3.5	30.3	238.22	8.6	C_3
	A 19		182	6.1	79.9	628.64	39.8	C_4–C_5
	A 21		294	9.8	164.6	1294.82	132.5	C_5
	A 17		371	12.4	133.3	1049.18	135.5	C_5
	A 18		476	15.9	169.5	1334.21	221.9	C_5+
	A 20		561	18.7	126.4	995.02	195.6	C_5+
	A 22		656	21.9	121.1	953.40	217.7	C_5+
ACS 3 Miranda	A 23		99	3.3	21.8	171.34	5.9	C_2
	A 24		176	5.9	24.6	193.36	11.8	C_2–C_3
	A 25		287	9.6	24.3	191.30	19.1	C_2–C_3
	A 26		364	12.1	19.8	155.69	19.7	C_2
	A 29		469	15.6	19.7	154.88	25.3	C_4–C_5
	A 27		554	18.5	22.3	175.80	35.2	C_5
	A 28		645	21.5	22.4	176.65	39.7	C_5

Table 7
Corrosion rate, thickness loss and atmosphere corrosivity degree – copper.

Corrosion site	Code	Photo after 21 months of exposure	Exposure time		Corrosion rate		Thickness loss (μm)	Corrosivity degree
			Days	Months	μm/year	(g/m^2 year)		
ACS 1 Alumar	C 16		104	3.5	3.4	30.78	1.0	C_5
	C 19		182	6.1	5.3	47.11	2.6	C_5
	C 21		294	9.8	8.0	71.52	6.4	C_5
	C 17		371	12.4	6.4	57.51	6.5	C_5
	C 18		476	15.9	5.1	45.52	6.6	C_5
	C 20		561	18.7	5.7	51.38	8.8	C_5
	C 22		656	21.9	4.7	42.00	8.4	C_5
ACS 3 Miranda	C 23		99	3.3	4.0	36.00	1.1	C_5
	C 24		176	5.9	4.3	38.78	2.1	C_5
	C 25		287	9.6	3.4	30.90	2.7	C_5
	C 26		364	12.1	2.9	25.86	2.9	C_5
	C 29		469	15.6	2.4	21.22	3.0	C_4
	C 27		554	18.5	4.0	36.29	6.2	C_5
	C 28		645	21.5	2.1	18.96	3.7	C_4

The average conditions observed for the climate and pollutant rates in Sao Luis area associated to the high time of wetness show an aggressive environment over the transmission line "Presidente Dutra". In ACS 1, the high settleable particulate matter reflects the highest corrosion rates in the area.

3.6. Mathematical model

The described artificial neural network model was used to predict corrosion of low-carbon steel, copper and aluminum under natural weathering in the region of São Luis–MA. For this type of analysis, more information had to be included in order to obtain significant results. For this reason, data sets from another two atmospheric corrosion stations [21–26], which are also in São Luis area, were considered. The total amount of corrosion data derive from 18 specimens of low-carbon steel, 17 specimens of copper and 16 specimens of aluminum. They were exposed for different periods in the ACS in São Luis area. In each period, environmental data were collected, along with particle deposition, pollutants concentrations and corrosion rates.

The neural network training, validation and test were performed three times for each metal. In each time three specimens were randomly separated from the group, which was used for training the network. After that, these separated specimens were used for validation and test.

Tables 9–11 show the network validation and test comparisons of calculated corrosion rates and laboratory corrosion evaluations for the three metals.

Low-carbon steel
Copper
Aluminum

The good correlations obtained in the analysis demonstrate the capacity of the proposed artificial neural network of learning to estimate the corrosion rate of low-carbon steel, copper and aluminum through the knowledge of specific environmental data in the region of São Luis. However, it must be emphasized that there is a short amount of available data sets, which makes it easier for the neural network to achieve such high correlation values.

In Table 11 an error over 50% in the prediction of the corrosion rate can be observed. One aspect which contributed to this high

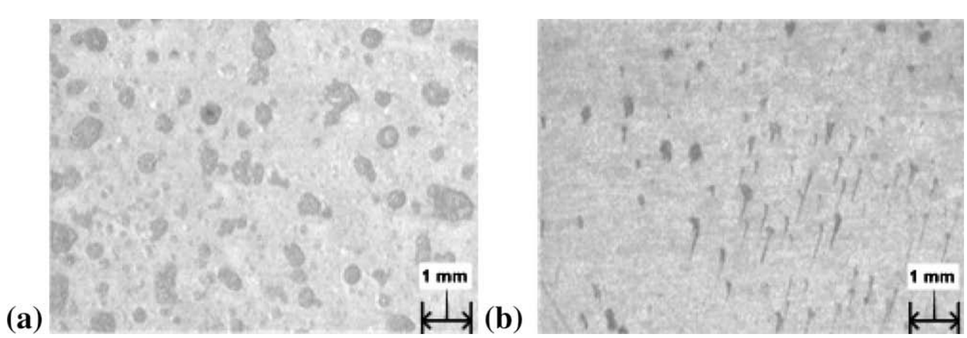

Fig. 11. OM micrographs showing wide and shallow pits on the copper surface after 21 months natural weathering: (a) ACS 1 Alumar; (b) ACS 3 – Miranda.

Table 8
Corrosion rate, thickness loss and atmosphere corrosivity degree – aluminum.

Corrosion site	Code	Photo after 21 months of exposure	Exposure Time		Corrosion rate		Thickness loss (µm)	Corrosivity degree
			Days	Months	(µm/year)	(g/m^2 year)		
ACS 1 Alumar	B 16		104	3.5	0.3	0.93	0.1	C_3
	B 19		182	6.1	1.3	3.54	0.6	C_4
	B 21		294	9.8	0.6	1.53	0.4	C_3
	B 17		371	12.4	0.5	1.39	0.5	C_3
	B 18		476	15.9	0.6	1.58	0.8	C_3
	B 20		561	18.7	0.6	1.53	0.9	C_3
	B 22		656	21.9	0.7	1.78	1.18	C_3
ECA_3 Miranda	B 23		99	3.3	0.1	0.24	>0.1	C_2
	B 24		176	5.9	0.2	0.65	0.1	C_3
	B 25		287	9.6	0.2	0.55	0.2	C_2
	B 26		364	12.1	0.1	0.33	0.1	C_2
	B 29		469	15.6	0.1	0.41	0.2	C_2
	B 27		554	18.5	0.1	0.39	0.2	C_2
	B 28		645	21.5	0.1	0.34	0.2	C_2

estimate error is the small range of the corrosion rates for the aluminum. Therefore, this error is not significant.

3.7. Long term corrosion rate prediction

Assuming that the amount of collected data is sufficient for training the artificial neural network, the following methodology is proposed for the long term corrosion rate prediction:

(a) With the knowledge of meteorological data and pollutants concentrations from a specific location were the metal specimens were (or are going to be) installed, the artificial neural network is used to predict corrosion rates for one and two years period. These values are represented by,

$$\left.\frac{dC}{dt}\right|_1 \text{ and } \left.\frac{dC}{dt}\right|_2 \tag{1}$$

and are calculated training the network separately with data of each period (1 year and 2 years). The decision about computing the corrosion rate for the period of two years is the necessity of introducing the environmental passivation effect, which, sometimes, is only perceived after one year [27]. Average environmental data values are used for each period.

(b) Assuming that corrosion evolution follows Pourbaix equation [28]: $C = k \cdot t^n$ where: C represents the average thickness loss of the metal in µm; t is the time of exposure in months or years; k and n are the constants obtained from the logarithmic linearization of this equation.

The constant k represents the corrosion in µm at the end of the first year of exposure; and the exponent n indicates the environmental passivation effect, which is directly dependent on the metal, the physical–chemical atmospheric conditions and the exposure conditions. These parameters are calculated with the following equations:

$$\frac{dC}{dt} = nkt^{n-1} \tag{2}$$

$$n = 1 + 0.477\left(\log\left(\left.\frac{dC}{dt}\right|_2\right) - \log\left(\left.\frac{dC}{dt}\right|_1\right)\right) \tag{3}$$

$$k = \frac{1}{n}\left.\frac{dC}{dt}\right|_1 \tag{4}$$

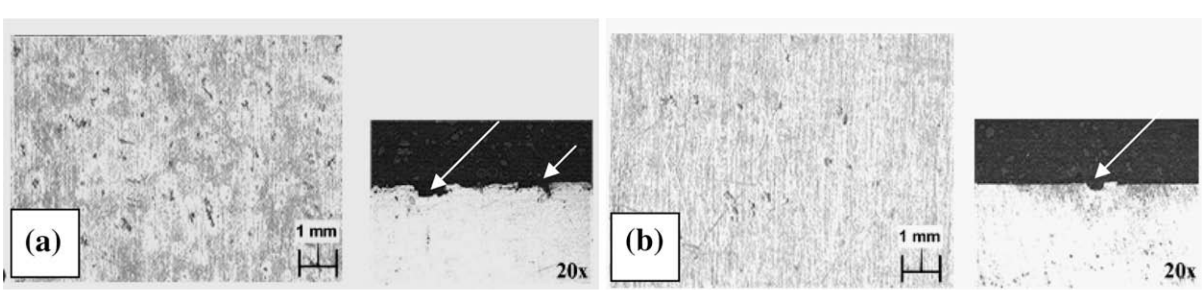

Fig. 12. OM micrographs showing pits on the aluminum surface after 21 months natural weathering: (a) ACS 1 Alumar; (b) ACS 3-Miranda.

Table 9
Low-carbon steel corrosion rate results with the training, validation and tests with the proposed neural network.

Specimen		Corrosion rate (μm/year)		
		Laboratory	Calculated	Error (%)
Validation 1	A 19	79.88	80.32	0.6
Validation 1	A 8	24.57	23.78	−3.2
Test 1	A 12	23.16	24.24	4.6
Obs: training correlation 0.9990				
Validation 2	A 18	169.53	169.46	0.0
Validation 2	A 29	19.68	20.59	4.6
Test 2	A 21	164.53	159.67	−3.0
Obs: training correlation 0.9970				
Validation 3	A 26	19.78	19.78	0.0
Test 3	A 23	21.77	19.06	−12.5
Obs: training correlation 0.9999				

Table 10
Copper corrosion rate results with the training, validation and test with the proposed neural network.

Specimen		Corrosion rate (μm/year)		
		Laboratory	Calculated	Error (%)
Validation 1	C 21	7.98	7.79	−2.3
Validation 1	C 3	4.56	4.58	0.4
Test 1	C 23	4.02	4.21	4.7
Obs: training correlation 0.9982				
Validation 2	C 16	3.44	3.44	0.0
Validation 2	C 25	3.45	3.45	0.0
Test 2	C 4	4.45	4.64	4.2
Obs: training correlation 0.9970				
Validation 3	C 18	5.08	5.08	0.0
Validation 3	C 5	5.26	5.26	0.0
Test 3	C 17	6.42	7.39	15.1
Obs: training correlation 0.9862				

Table 11
Aluminum corrosion rate results with the training, validation and test with the proposed neural network.

Specimen		Corrosion rate (μm/year)		
		Laboratory	Calculated	Error (%)
Validation 1	B 16	0.344	0.344	0.0
Test 1	B 5	0.582	0.487	−16.3
Obs: training correlation 0.9997				
Validation 2	B 21	0.564	0.564	0.0
Validation 2	B 25	0.203	0.203	0.0
Test 2	B 27	0.145	0.154	6.3
Obs: training correlation 1.0000				
Validation 3	B 19	1.309	1.309	0.0
Validation 3	ALU 10	1.298	1.298	0.0
Test 3	B 23	0.087	0.137	56.5
Obs: training correlation 0.9997				

Therefore, with the knowledge of environmental conditions of a certain location, corrosion parameters k and n can be calculated, once the neural network is applied to estimate the corrosion rates at this location.

(c) Prediction of corrosion with Pourbaix equation [28]. Pourbaix equation parameters for ACS 1 and ACS 3 were calculated and are listed in Table 12, for each analyzed metal.

In Figs. 13–15, the obtained Pourbaix equations with parameters derived from the neural network analysis, for each metal, are plotted and compared to the experimental data of thickness loss measured in laboratory from the collected specimens. In general, good agreement can be observed in the graphs for the 2 years period.

These equations can also be used for long term predictions (over 2 years). However, it is suggested the inclusion of further experimental data to enrich the neural network training.

Table 12
Pourbaix equation parameters for low-carbon steel, copper and aluminum at Alumar and Miranda sites.

ACS	Low-carbon steel		Copper		Aluminum	
	n	k	n	k	n	k
ACS 1_Alumar	1.55	71.25	0.72	8.43	0.58	1.12
ACS 3_Miranda	0.86	22.13	1.12	2.88	1.02	0.17

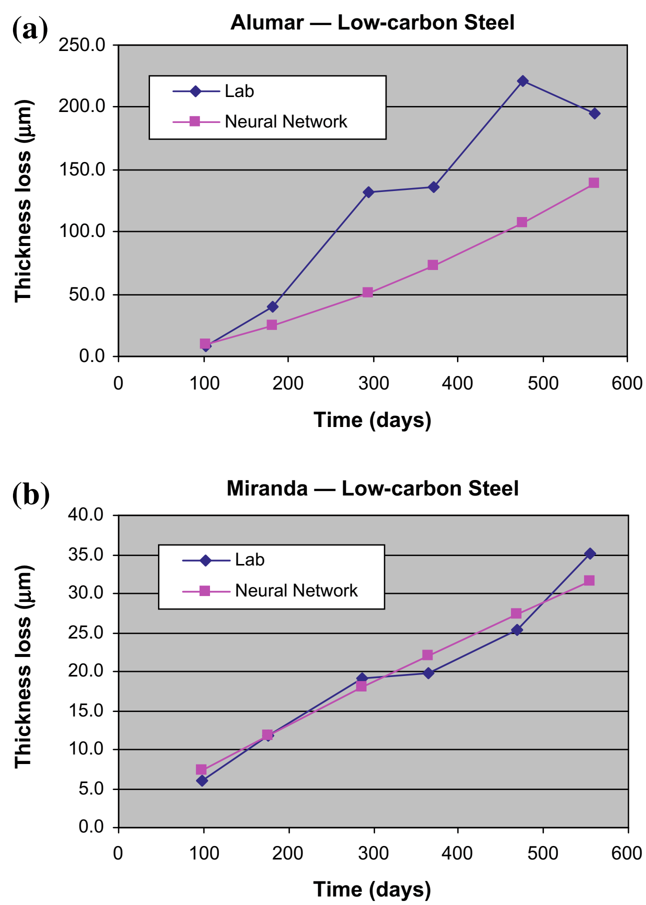

Fig. 13. Thickness loss of low-carbon steel along time- comparison of experimental data (Lab) and numerical data (Neural Network): (a) ACS 1 – Alumar; (b) ACS 3 – Miranda.

4. Conclusions

Artificial neural networks have emerged as a powerful tool for the prediction of corrosion processes in metals under natural weathering conditions. In this work, a feedforward artificial neural network model has been selected and trained with corrosion data collected from sites along the “702 – São Luis – Presidente Dutra” transmission line. In this training, analytical weights are defined in order to correlate several sets of environmental and pollutant parameters with corresponding corrosion values in three types of metals in different periods.

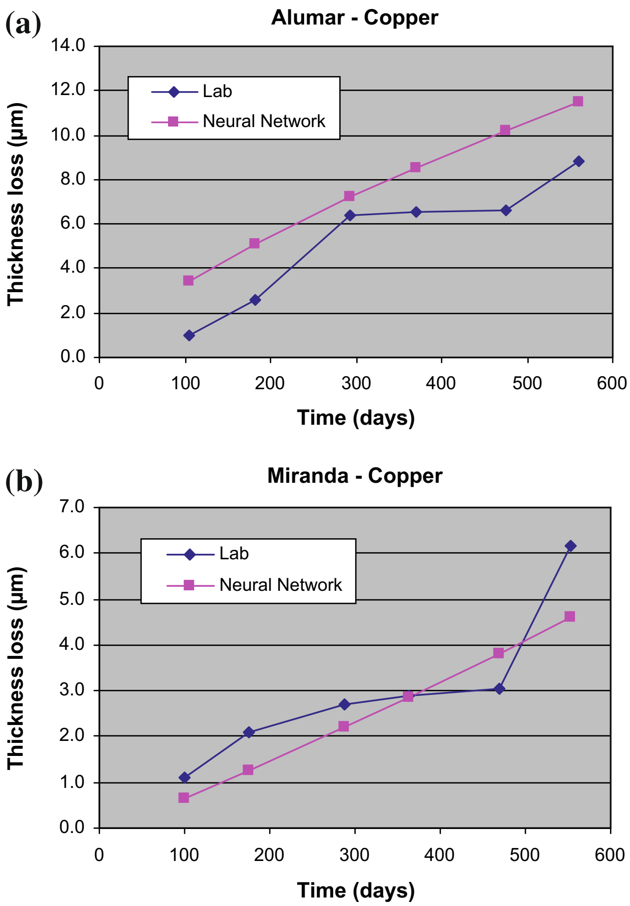

Fig. 14. Thickness loss of copper along time- comparison of experimental data (Lab) and numerical data (Neural Network): (a) ACS 1 – Alumar; (b) ACS 3 – Miranda.

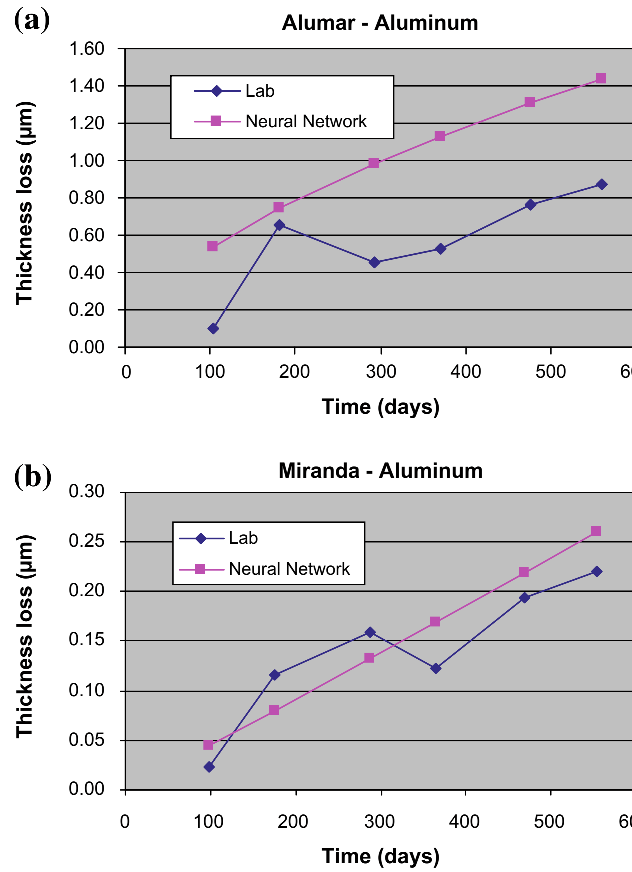

Fig. 15. Thickness loss of aluminum along time – comparison of experimental data (Lab) and numerical data (Neural Network): (a) ACS 1 – Alumar; (b) ACS 3 – Miranda.

The adopted network for the corrosion estimate analysis is a perceptron multilayer model with the following characteristics: 10 neurons in the entry layer, one for each environmental parameter (time of exposure, temperature, relative humidity, precipitation, time of wetness, wind velocity, solar radiation, chloride ions, sulfur compounds and dustfall); two intermediate layers of sigmoidal neurons – the first layer with tangential modulating functions and the second layer with logarithmic modulating functions. In that way, the signal passed to the last layer is a positive number between 0 and 1; one output neuron with a linear function (*purelin*) to amplify the received signal to real corrosion rate values. The backpropagation algorithm used for training the network was Levenberg–Marquardt, which presented the best performance in the search for the weights for the neuron connectors.

Data from four corrosion stations were used to train, validate and test the model. The comparisons between experimental values and numerical results were generally good suggesting that the model can be used to estimate corrosion in the São Luis area. Despite all these results, it is important to increase the number of experimental data sets to obtain higher confidence and more representative results.

Given the versatility of the neural network technique, with further and varied input data sets this model may also be used to estimate corrosion in other areas.

Acknowledgements

The authors would like to thank Companhia Energética do Maranhão – CEMAR (Maranhão Energy Company), Centrais Elétricas do Norte, ELETRONORTE (Northern Electricity Center), ANEEL and UFPR/PIPE for their technical and financial support, as well as the academic opportunity for developing this work.

References

[1] E.D. Kenny, E.J. Esmanhoto, Tratamento estatístico do desempenho de materiais metálicos no estado do Paraná, in: XVII Congresso Brasileiro de Corrosão, Rio de Janeiro, Anais, ABRACO, T-24, 1993, pp. 297–308.
[2] E.D. Kenny, E.J. Esmanhoto, Corrosão do aço-carbono por intemperismo natural no Estado do Paraná, in: IV Seminário de Materiais no Setor Elétrico, Curitiba, Anais, Copel/UFPR, 1994, pp. 377–382.
[3] S. Feliu, M. Morcillo, S. Feliu Jr., The prediction of atmospheric corrosion from meteorological and pollution parameters-I. Annual corrosion, Corrosion Science 34 (1993) 403–414.
[4] S. Feliu, M. Morcillo, S. Feliu Jr., The prediction of atmospheric corrosion from meteorological and pollution parameters-II. Long-term forecasts, Corrosion Science 34 (1993) 415–422.
[5] L. Mariaca, M. Morcillo, Funciones de daño (dosis/respuesta) de la corrosion atmosferica en Iberoamerica: Programa CYTED. Seccion B-7, Gráficas Salué, Madrid, 1998. pp. 629–660.
[6] S. Pintos, N.V. Queipo, O.T. Rincón, A. Rincón, M. Morcillo, Artificial neural network modelling of atmospheric corrosion in the MICAT project, Corrosion Science 42 (2000) 35–52.
[7] I. Helliwell, M. Turega, R. Cottis, Neural networks for corrosion data reduction, en: Corrosion 96, Denver, USA, 1996, p. 739.
[8] O.T. Rincón, Tratamiento mediante una red neuronal artificial de los datos de corrosión atmosférica obtenidos: programa CYTED. Seccion B-8, Gráficas Salué, Madrid, 1998. pp. 661–677.
[9] D.T. Pham, X. e LIU, Neural Networks for Identification, Prediction and Control, Springer-Verlag, London, 1995. 238 p.
[10] A.P. Braga, T.B. Ludemir, A.C.P.F. Carvalho, Redes neurais artificiais – teoria e aplicações, Rio de Janeiro, LTC Livros Técnicos e Científicos Editora S.A., 2000, 237 p.
[11] M.I.P. de Camargo Libos, Dissertação de Mestrado, Universidade Federal do Rio de Janeiro, Brazil, 2002.
[12] L.K.S. Santos, Treinamento em ArcView GIS 8.3 básico, Apostila do Curso de Especialização em Geoprocessamento – Universidade Federal do Paraná, CIEG – Centro integrado de estudos em geoprocessamento, Curitiba 2005, 141 p.

[13] ASSOCIAÇÃO BRASILEIRA DE NORMAS TÉCNICAS, NBR 6211: determinação de cloretos na atmosfera pelo método da vela úmida, Rio de Janeiro, 2001.
[14] ASSOCIAÇÃO BRASILEIRA DE NORMAS TÉCNICAS, NBR 6921: sulfatação total na atmosfera – determinação da taxa pelo método da vela de dióxido de chumbo, Rio de Janeiro, 1981.
[15] American Society for Testing and Materials, ASTM D 1739: Standard test method for collection and measurement of dustfall (Settleable Particulate Matter), 1994.
[16] ASSOCIAÇÃO BRASILEIRA DE NORMAS TÉCNICAS, NBR 6209: materiais metálicos não revestidos – ensaio não acelerado de corrosão atmosférica, Rio de Janeiro, 1986, 5 p.
[17] CENTRO DE PREVISÃO DE TEMPO E CLIMA – CPTEC. Disponível em www.cptec.inpe.br, acessada em Março de, 2006.
[18] ASSOCIAÇÃO BRASILEIRA DE NORMAS TÉCNICAS, NBR 14643: corrosão atmosférica – classificação da corrosividade de atmosferas, Rio de Janeiro, 2001.
[19] M. Morcillo, E. Almeida, B. Rosales, J. Uruchurtu, M. Marrocos, Corrosión y protección de metales en las atmósferas de Iberoamerica: programa CYTED, Gráficas Salué, Madrid, 1998.
[20] ASSOCIAÇÃO BRASILEIRA DE NORMAS TÉCNICAS, NBR 6210: preparo, limpeza e avaliação da taxa de corrosão de corpos-de-prova em ensaios de corrosão atmosférica, Rio de Janeiro, 1982.
[21] E.D. Kenny, O.M. Cruz, J.M. Silva, Y.C. Sica, M. Ravaglio, P.R. Mendes, J.C. Mendes, Desenvolvimento de metodologia para monitoramento do grau de poluição nos alimentadores de 13.8 kV e 69 kV da ilha de São Luís, Curitiba: LACTEC, Relatório técnico, 98 p.
[22] E.D. Kenny, Y.C. Sica, O.M. Cruz, J.M. Silva, J. Lázaris, J.V.N. Junior, M. Ravaglio, P.R. Mendes, J.C. Mendes, O impacto da poluição atmosférica sobre a rede aérea de distribuição de energia da Ilha de São Luís, in: II CITENEL – Congresso de inovação tecnológica em energia elétrica, 2003, Salvador, Anais, ANEEL – Universidade de Salvador, vol. I, 2003, pp. 561–566.
[23] E.D. Kenny, Y.C. Sica, O.M. Cruz, J.M. Silva, M. Ravaglio, P.R. Mendes, J.C. Mendes, J. Junior, Desenvolvimento de metodologia para monitoramento do grau de poluição nos alimentadores de 13.8 kV e 69 kV da Ilha de São Luís, in: 7ª COTEQ – Conferência sobre tecnologia de equipamentos, 2003, Florianópolis, Anais, 2003.
[24] E.D. Kenny, Y.C. Sica, O.M. Cruz, P.R. Mendes, J.C. Mendes, M. Ravaglio, W.A. Kapp, Desenvolvimento de metodologia para monitoramento do grau de poluição nos alimentadores de 13.8 kV e 69 kV da Ilha de São Luís – parte II, in: III CITENEL, 2005, Florianópolis. Congresso de inovação tecnológica em energia elétrica, 2005.
[25] E.D. Kenny, Y.C. Sica, O.M. Cruz, M. Ravaglio, A.T. Calmón, Mapeamento da corrosividade atmosférica da ilha de São Luís, in: LATINCORR – Congresso Latino Americano de Corrosão, 2006, Fortaleza – Brazil, Anais, 2006.
[26] E.D. Kenny, Y.C. Sica, K.F. Portella, D.F. C FILHO, Atmospheric corrosion performance of carbon steel, galvanized steel, aluminum and copper in the north Brazilian coast, Journal of the Brazilian Chemical Society, Brazil, 18 (N.1) (2007) 153–166.
[27] P.R. Roberge, R.D. Klassen, P.D. Haberecht, Atmospheric corrosivity modelling – a review, Materials and Design 23 (2002) 321–330.
[28] M. Pourbaix, International cooperation in the prevention of corrosion of materials, in: IX International Congress of Metallic Corrosion, Florença, Itália, Anais, 1990.